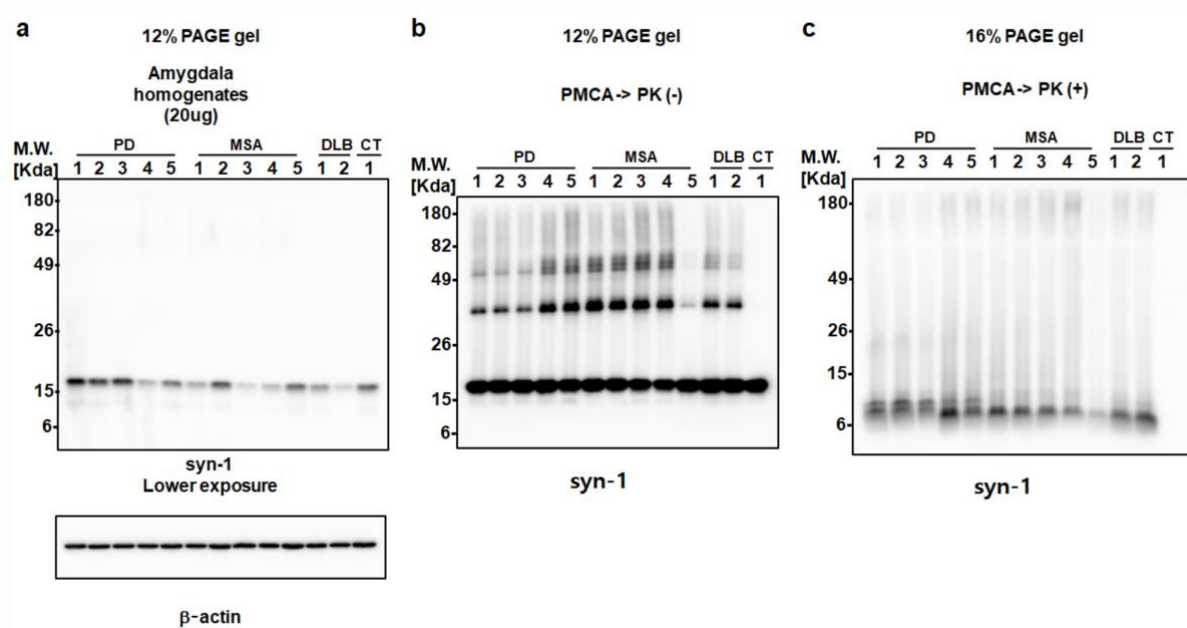


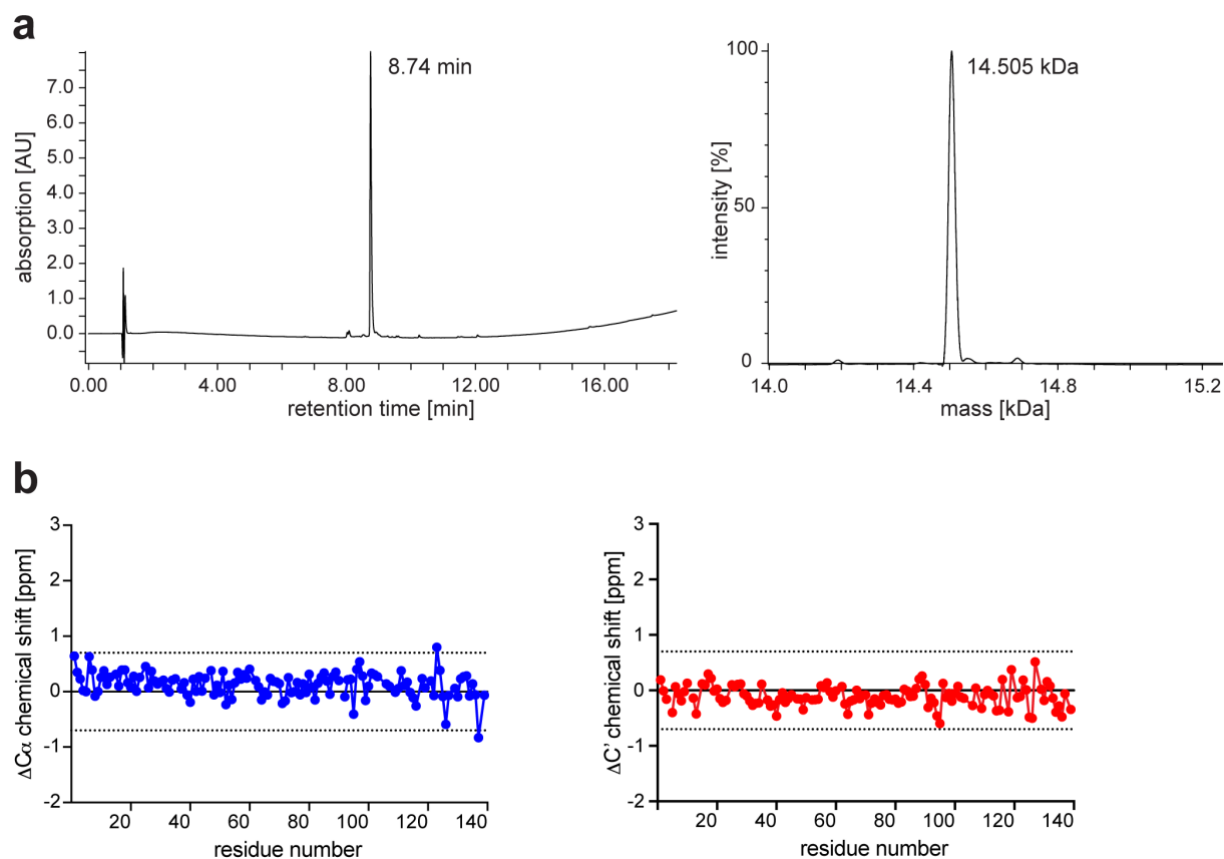
## **Supplementary Information**

### **Structural heterogeneity of $\alpha$ -synuclein fibrils amplified from patient brain extracts**

Timo Strohäker et al.

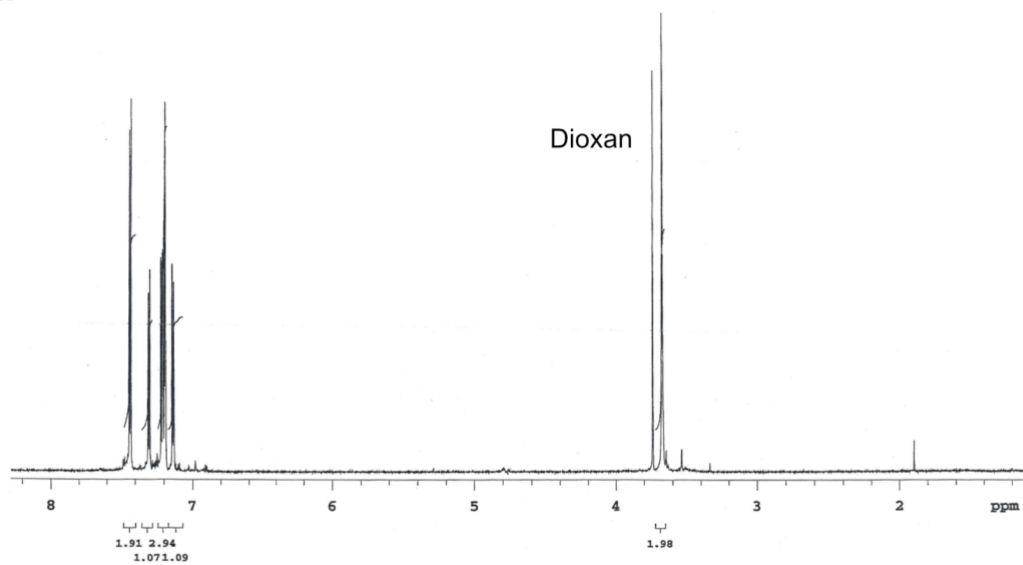


**Supplementary Fig. 1 Amplification of aSyn fibrils from brain extracts.** **a**, Immunoblotting of brain extracts (CT; brain extract from an individual, in which a synucleinopathy was excluded). The degree of aSyn expression level was not directly correlated with synucleinopathies. **b**, Immunoblotting of PMCA products with indicated brain extracts as seeds. High-molecular weight aSyn was induced through PMCA with patient brain extracts, whereas control brain extract failed to induce high-molecular weight aSyn after PMCA. **c**, Immunoblotting of PMCA products with proteinase-K (PK) digestion. PK-resistant signals were detected in samples from patients pathologically confirmed with a synucleinopathy, whereas nothing remained in the control sample.

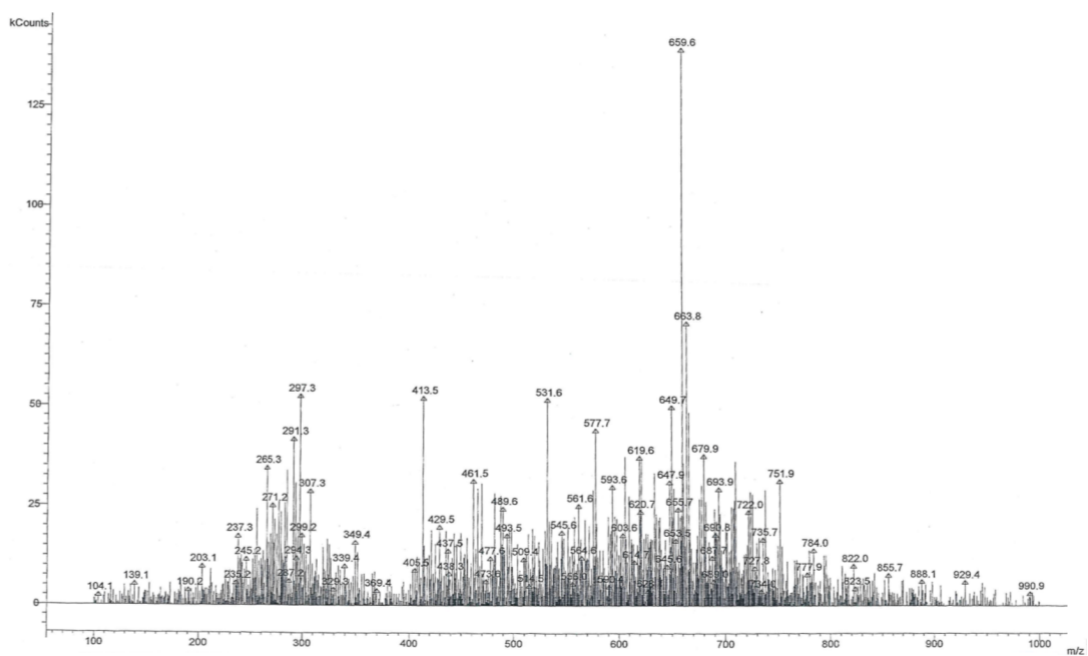


**Supplementary Fig. 2 aSyn is disordered in fibril dissociation buffer. a**, Mass spectrum of N-terminally acetylated aSyn. **b**,  $C\alpha$  and  $C'$  secondary chemical shifts of N-terminally acetylated aSyn in the dissociation buffer (4M GdSCN, 0.4 % formic acid, pH 2.5). Because secondary chemical shifts are small, aSyn does not contain hydrogen-bonded secondary structure in the fibril dissociation buffer.

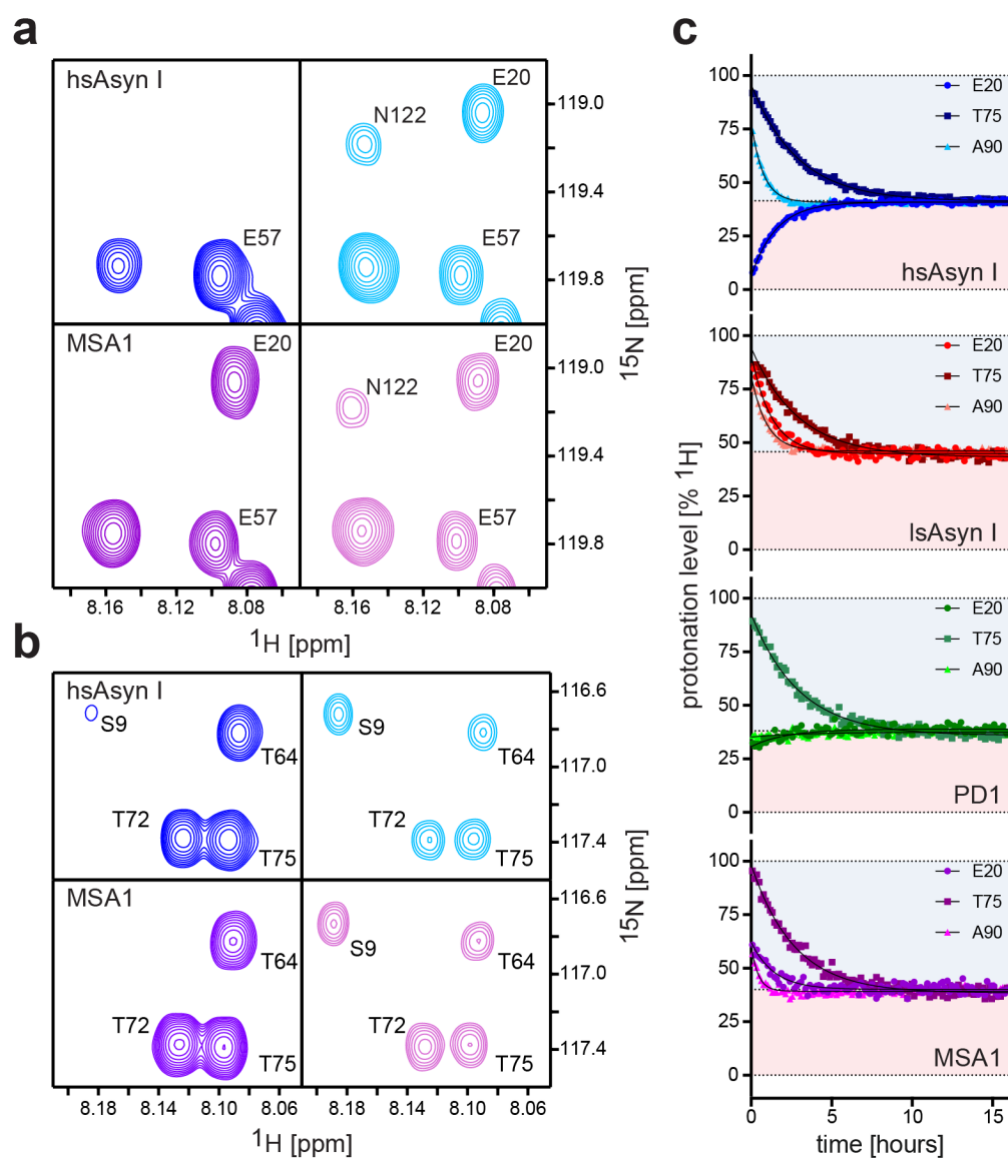
**a**



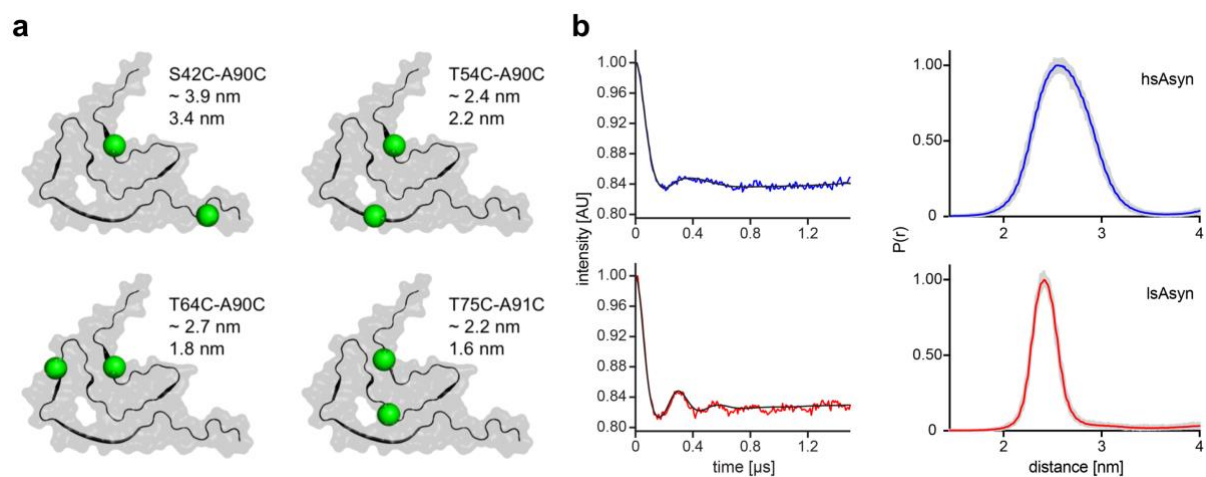
**b**



**Supplementary Fig. 3** <sup>1</sup>H NMR spectrum (a) and mass spectrum (b) of HS-68.



**Supplementary Fig. 4 HD exchange NMR data of different aSyn fibrils. a,b,** Selected regions from  $^1\text{H}$ - $^{15}\text{N}$  correlation spectra recorded after fibril dissociation at the beginning (left) and end (right) of the back-exchange period for the hsAsyn polymorph (top) and aSyn fibrils amplified from the brain extract of a MSA patient (bottom). **c,** Time-dependent back exchange of selected residues for different aSyn fibril types (from top to bottom; Table 1): hsAsyn, lsAsyn, PD1, MSA1.



**Supplementary Fig. 5 EPR PELDOR measurements.** **a**, Distances measured by PELDOR for four MTSL-pairs in the *in vitro* high-salt polymorph of aSyn (upper values; Pornsuwan et al. *Angew Chem* 2013) in comparison to the cryo-electron microscopy structure (lower values; C $\alpha$ -C $\alpha$  distances in PDB code: 6A6B). Changes in the orientation of the MTSL-side chain were previously estimated to amount to ~0.4-0.5 nm, so could reach ~1 nm for a MTSL-pair. **b**, Dipolar modulation (left; corrected for background; fit in blue/red) and normalized distance distributions (right) determined by artificial neuronal network analysis implemented in DeerAnalysis2018 for hsAsyn (top, blue) and lsAsyn (bottom, red).

---

**aSyn T54C mutation forward primer**

5`-GAG TGG TGC ATG GTG TGG CAT GCG TGG CTG AGA AGA CCA AAG-3`

**aSyn T54C mutation reverse primer**

5`-CTT TGG TCT TCT CAG CCA CGC ATG CCA CAC CAT GCA CCA CTC-3`

---

**aSyn A90C mutation forward primer**

5`-GGA GCA GGG AGC ATT GCA TGT GCC ACT GGC TTT GTC AAA AAG-3`

**aSyn A90C mutation reverse primer**

5`-CTT TTT GAC AAA GCC AGT GGC ACA TGC AAT GCT CCC TGC TCC-3`

---

**Supplementary Table 1 QuikChange Primer.**